Electronic Supplementary Material (ESI) for RSC Advances.

Experimental and theoretical study on converting myoglobin into a stable domain-swapped dimer by utilizing a tight hydrogen bond network at the hinge region

Cheng Xie[a], Hiromitsu Shimoyama[b], Masaru Yamanaka[a], Satoshi Nagao‡[a], Hirofumi Komori[c], Naoki Shibata[d], Yoshiki Higuchi[d], Yasuteru Shigeta[*b], and Shun Hirota[*a]

[a]*Division of Materials Science, Graduate School of Science and Technology, Nara Institute of Science and Technology, 8916-5 Takayama, Ikoma, Nara 630-0192, Japan. E-mail: hirota@ms.naist.jp.*
[b]*Division of Life Science, Center for Computational Sciences, University of Tsukuba, 1-1-1, Tennodai, Ibaraki, 305–8577 Japan. E-mail: shigeta@ccs.tsukuba.ac.jp.*
[c]*Faculty of Education, Kagawa University, 1-1 Saiwai-cho, Takamatsu, Kagawa 760-8522, Japan.*
[d]*Graduate School of Science, University of Hyogo, 3-2-1 Koto, Kamigori-cho, Ako-gun, Hyogo 678-1297, Japan.*

‡Present address: Graduate School of Science, University of Hyogo, 3-2-1 Koto, Kamigori-cho, Ako-gun, Hyogo 678-1297, Japan.

Table of Contents

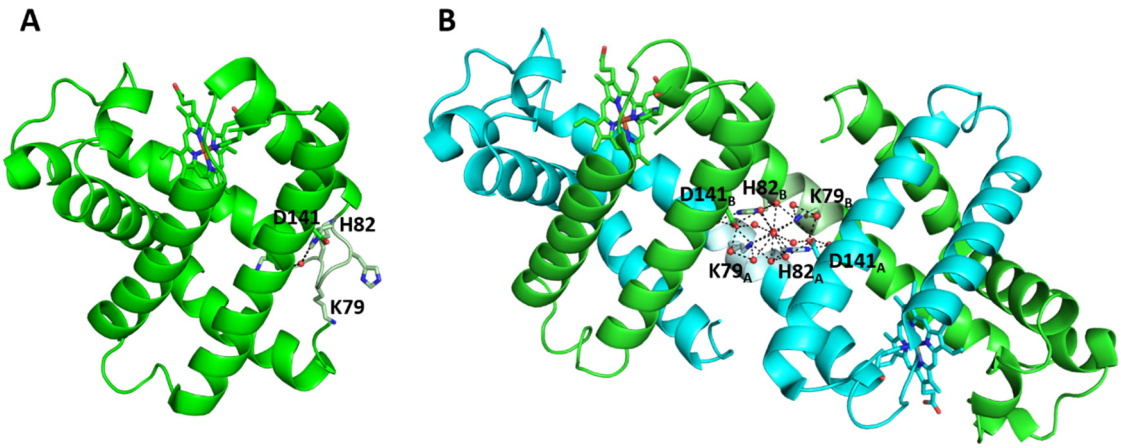

Fig. S1. Crystal structures WT Mb (A) monomer (PDB ID: 1WLA) and (B) dimer (PDB ID: 3VM9). The monomer is shown in green, whereas the two protomers of the dimer are shown in green and cyan. The hinge region is shown in pale colours. The side-chain atoms of residues K79, H82, and D141 and the hemes are shown as stick models. Water molecules are depicted as red spheres. The H-bonds involving K79, H82, D141, or a water molecule at the hinge region are shown as dotted lines.

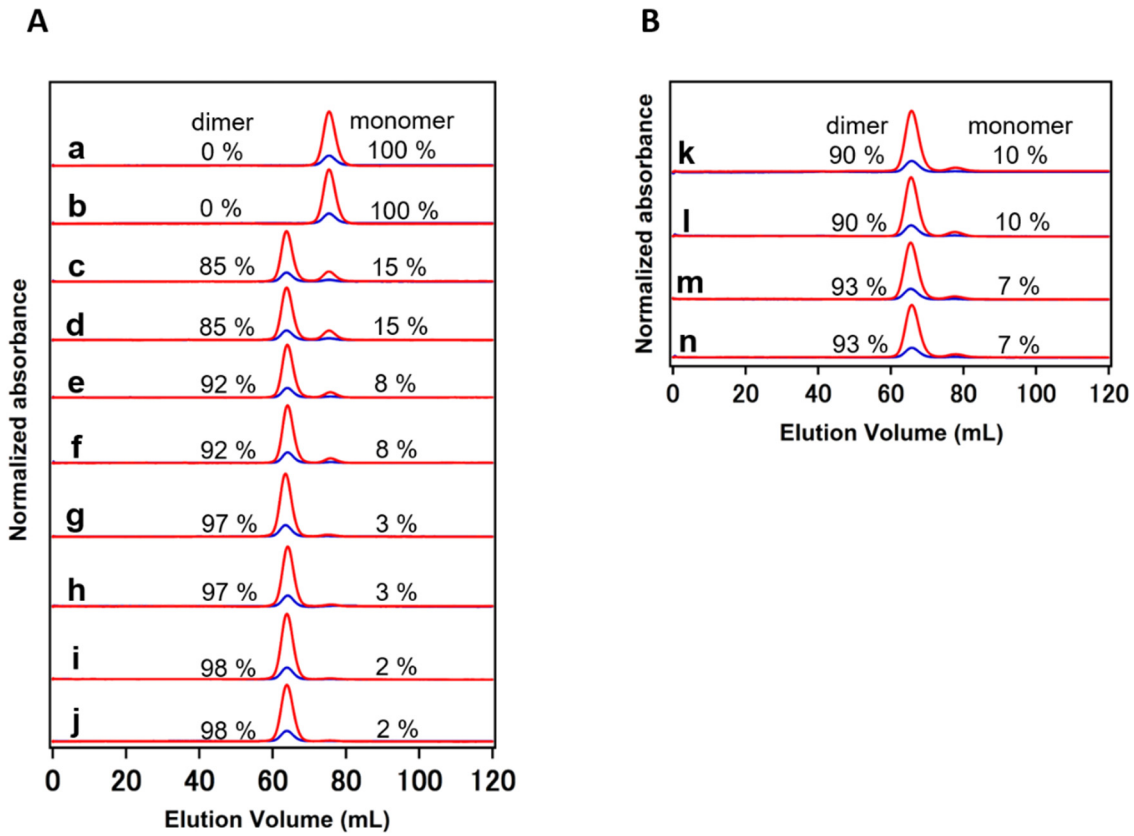

Fig. S2. Size exclusion chromatography elution curves of WT and mutant Mbs: (a, b) WT, (c, d) K_3A_3, (e, f) K_3A_2H, (g, h, k, l) K_3A_2H-L137E, and (i, j, m, n) K_3A_2H-L137D Mb. Elution curves after heating the monomer (a, c, e, g, i, k, m) and dimer (b, d, f, h, j, l, n) at 70 °C for (a, b, e, f, g, h, i, j) 30 min and (c, d, k, l, m, n) 60 min are shown. The intensities of the curves are normalized by the total area of the curve. Measurement conditions: Mb concentration, (A) 100 μM (heme unit), (B) 5 μM (heme unit); column, HiLoad 16/60, Superdex 75 pg; detection wavelength, 280 nm (blue) and 408 nm (red); buffer, 50 mM potassium phosphate buffer, pH 7.0; temperature, 4 °C.

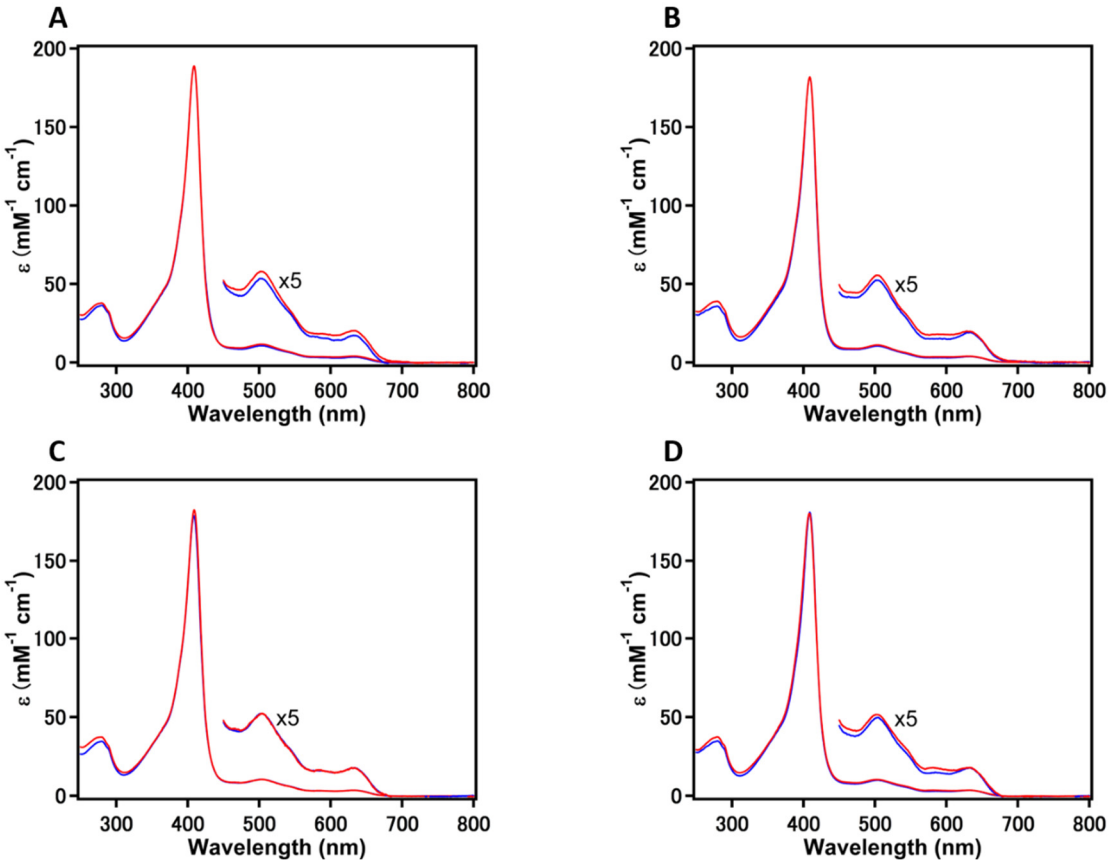

Fig. S3. Optical absorption spectra of WT and mutant Mbs in their met forms: (A) WT, (B) K_3A_2H, (C) K_3A_2H-L137E, and (D) K_3A_2H-L137D Mb. The spectra of the Mb monomer (blue) and dimer (red) are shown. Measurement conditions: solution condition, 50 mM potassium phosphate buffer, pH 7.0; path length, 10 mm; temperature, 25 °C.

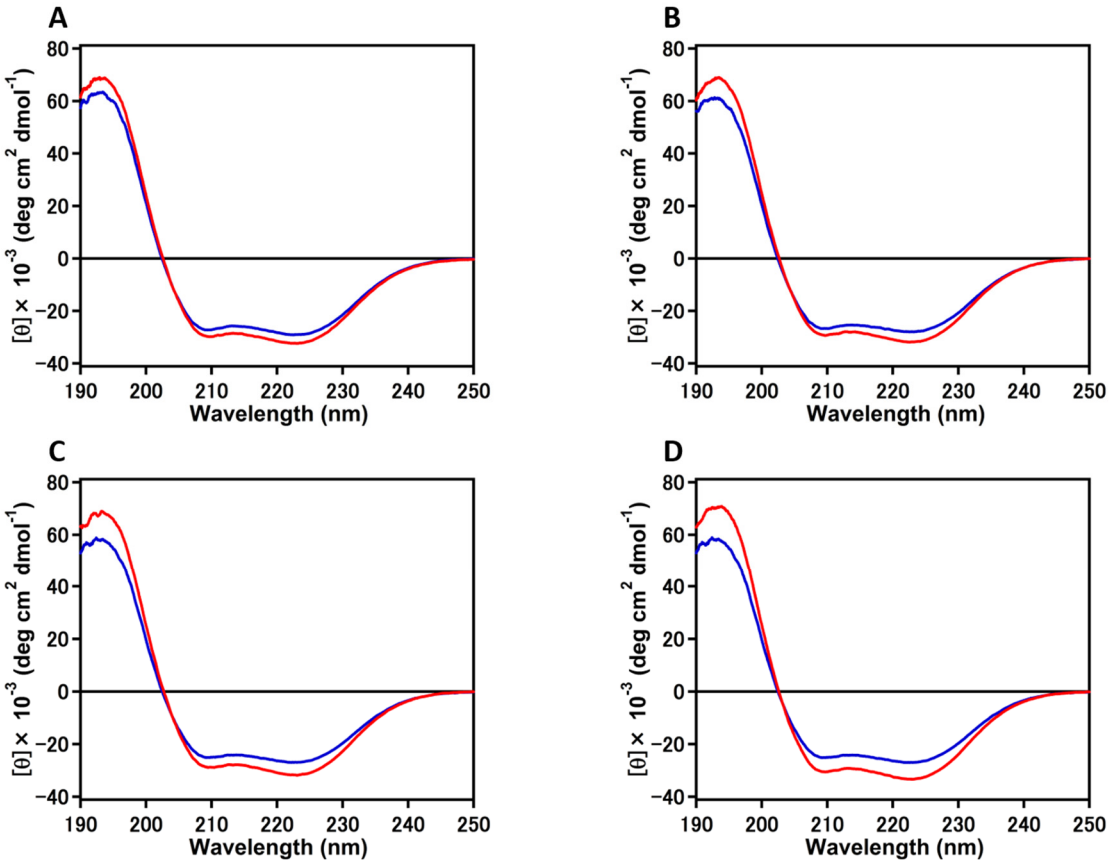

Fig. S4. CD spectra of WT and mutant Mbs in their met forms: (A) WT, (B) K_3A_2H, (C) K_3A_2H-L137E, and (D) K_3A_2H-L137D Mb. The spectra of the Mb monomer (blue) and dimer (red) are shown. Measurement conditions: Mb concentration, 5~6 μM (heme unit); solution condition, 50 mM potassium phosphate buffer, pH 7.0; path length, 1 mm; temperature, 25 °C.

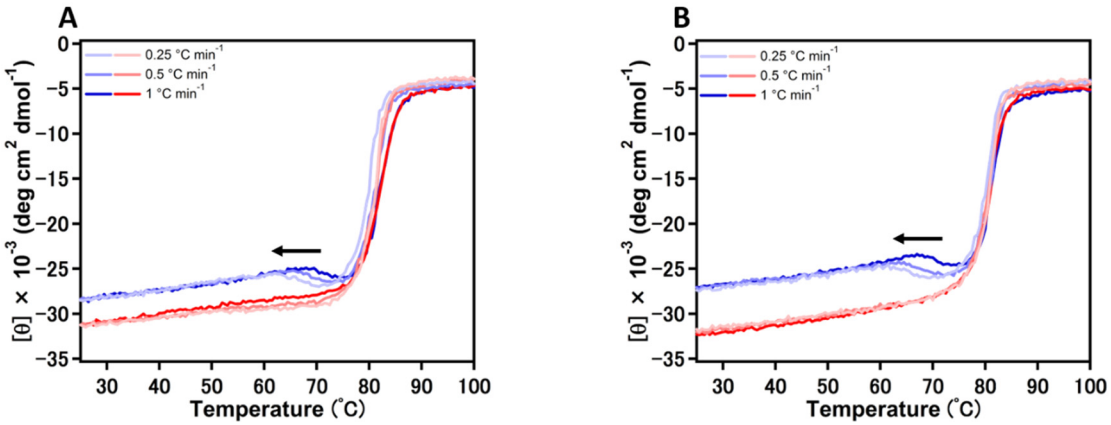

Fig. S5. CD ellipticity changes at 222 nm with temperature for K_3A_2H-L137E and K_3A_2H-L137D Mb in their met forms: (A) K_3A_2H-L137E and (B) K_3A_2H-L137D Mb. The changes in the Mb monomer (blue) and dimer (red) are shown. Measurement conditions: Mb concentration, 30~33 μM (heme unit); solution condition, 50 mM potassium phosphate buffer, pH 7.0; path length, 1 mm; temperature, 25-100 °C; scan rate, 0.25, 0.5, or 1 °C min^{-1}.

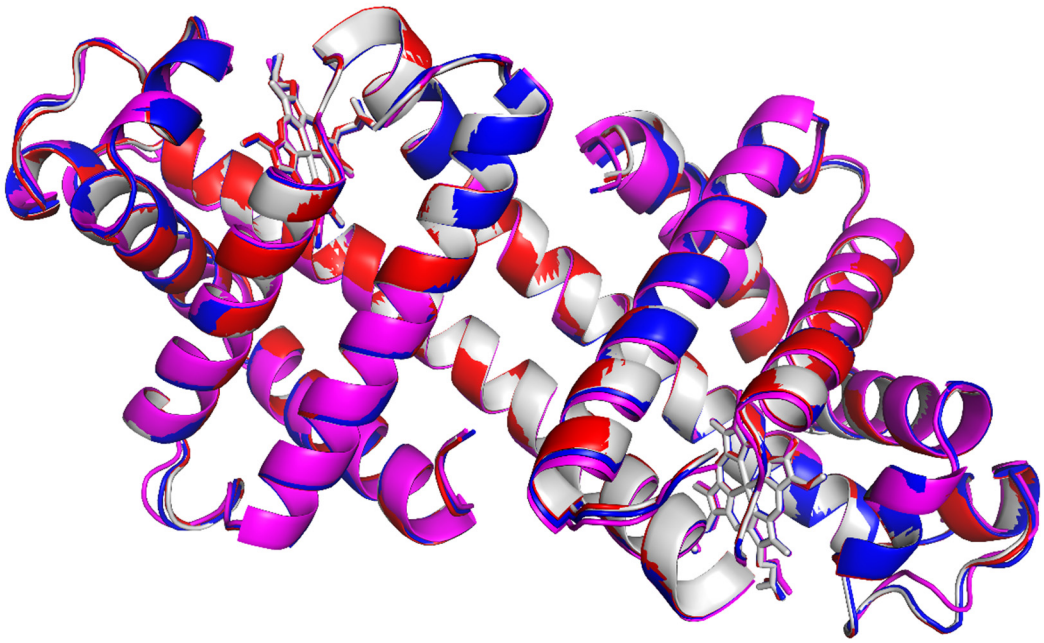

Fig. S6. Superimposed structures of WT and mutant Mb dimers: WT (gray), K_3A_2H (red), K_3A_2H-L137E (blue), and K_3A_2H-L137D Mb (magenta). The hemes are shown as stick models.

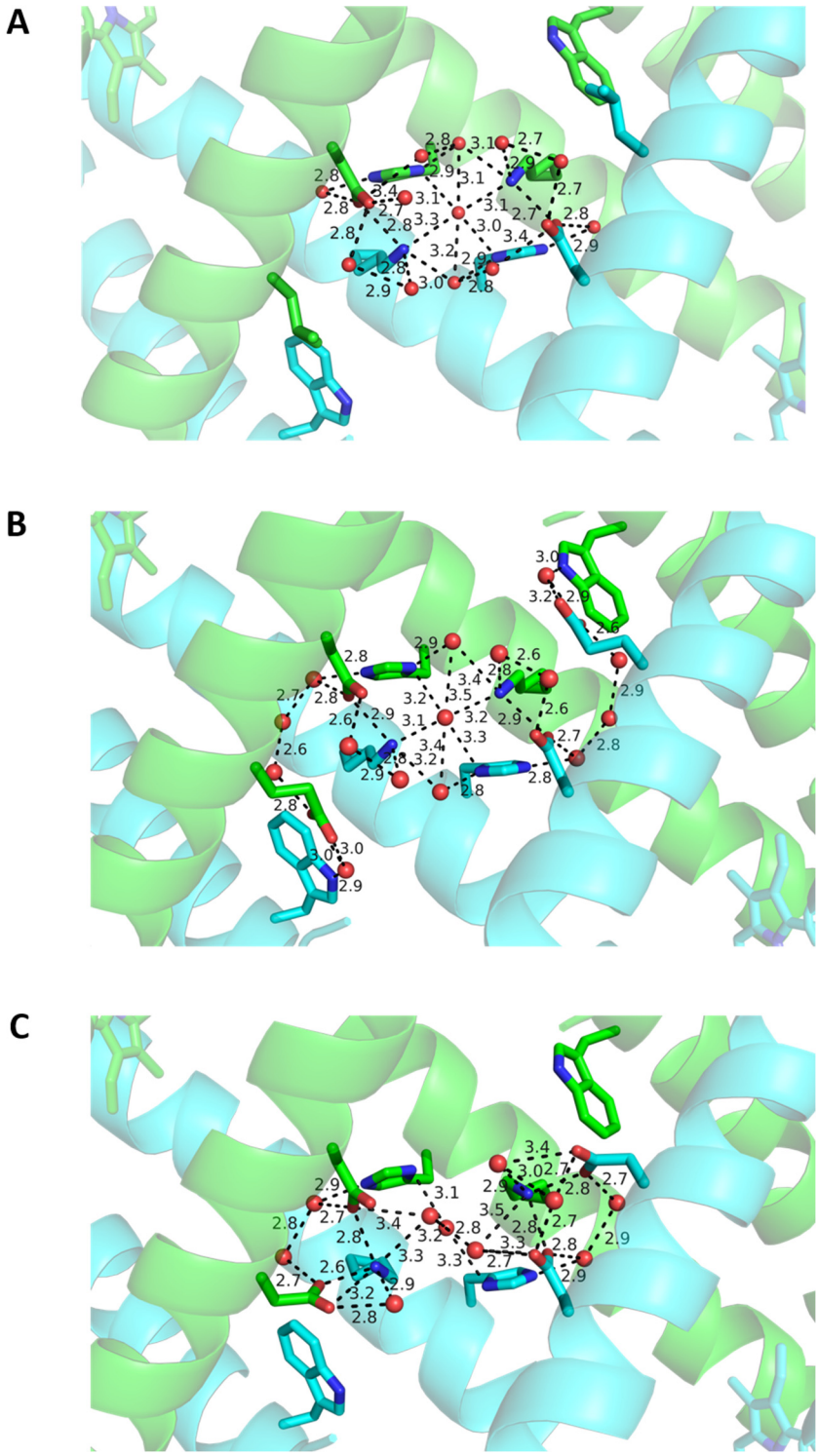

Fig. S7. Distances of H-bonds in (A) K_3A_2H, (B) K_3A_2H-L137E, and (C) K_3A_2H-L137D Mb dimers. The two protomers are shown in green and cyan. The side-chain atoms of residues W7, K79, H82, L137/E137/D137, and D141 and the hemes are shown as stick models. Water molecules are depicted as red spheres. The H-bond network involving W7, K79, H82, L137/E137/D137, D141, and water molecules at the hinge region are shown as dotted lines. Distance unit: Å.

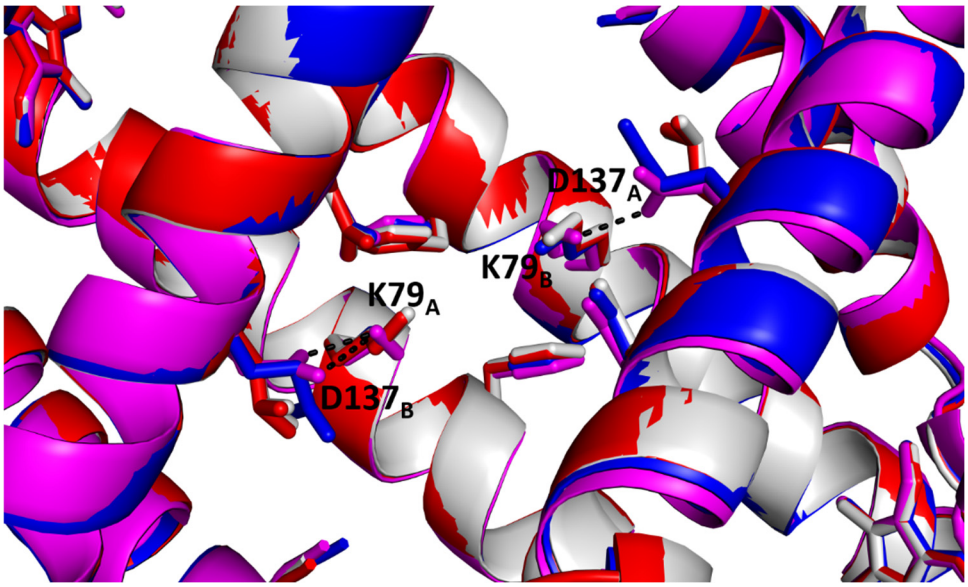

Fig. S8. Superimposed structures of the hinge region of WT and mutant Mb dimers: WT (gray), K_3A_2H (red), K_3A_2H-L137E (blue), and K_3A_2H-L137D Mb (magenta). The K79, H82, L137/E137/D137, and D141 and hemes are shown as stick models. The H-bonds between K79 and D137 are shown as dotted lines. A and B in the residue number represent each protomer.

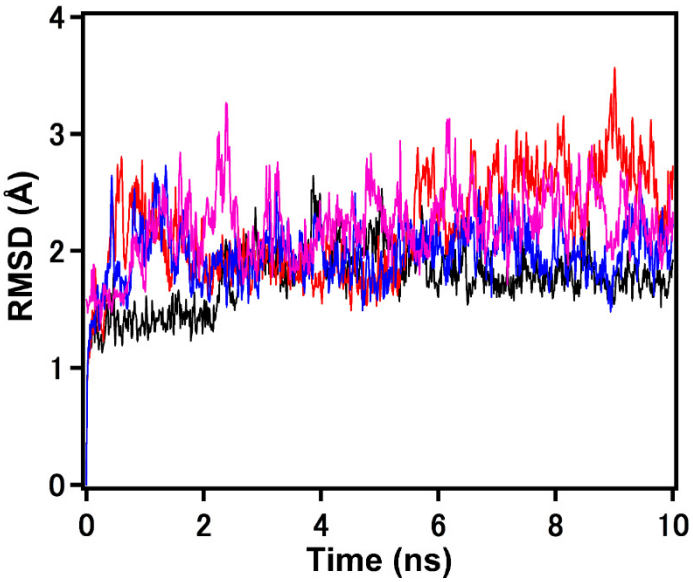

Fig. S9. Trajectories of the root-mean-square-distance (RMSD) of WT (black), K_3A_2H (red), K_3A_2H-L137E (blue) and K_3A_2H-L137D Mb dimer (magenta).

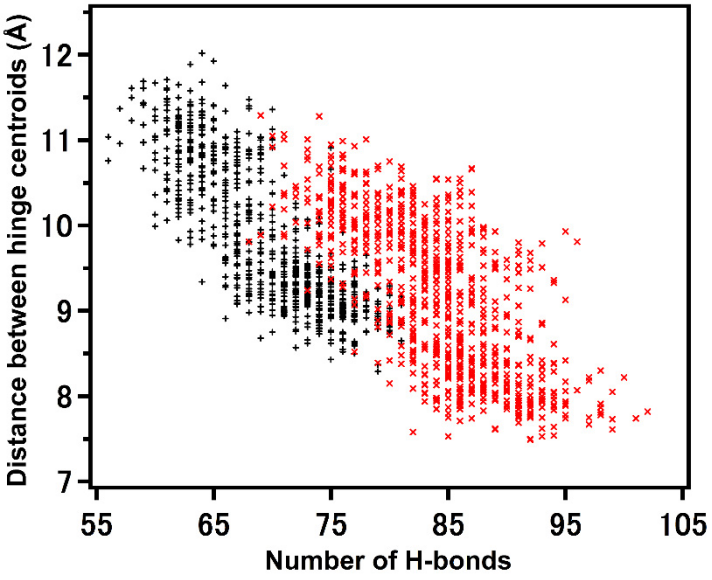

Fig. S10. Scatter plot of the number of H-bonds (x-axis) and the distance between hinge centroids (y-axis). The black and red points represent the WT and K_3A_2H Mb dimer distributions, respectively.

Table S1. Nucleotide sequences of the primers

Primer	Sequence [a]
G80A/H81A-F	GCCCACGAAGCTGAGCTCAAACC
G80A/H81A-R	CGCTTTTTTCTTAAGGATGCCACCTAGG
L137E-F	GAATTCCGTAACGATATCGCTGCTAAG
L137E-R	CTCGAGAGCTTTGGTCATAGCAC
L137D-F	GATTTCCGTAACGATATCGCTGCTAAG
L137D-R	CTCGAGAGCTTTGGTCATAGCAC (same to L137E-R)

[a] Underlines indicate the replaced nucleotides.

Table S2. Statistics of data collection and structure refinement of K_3A_2H, K_3A_2H-L137E, and K_3A_2H-L137D Mb dimers.

	K_3A_2H Mb dimer	**K_3A_2H-L137E Mb dimer**	**K_3A_2H-L137D Mb dimer**
Data collection	20181026	20210214	20210622
X-ray source	SPring-8 (BL38B1)	SPring-8 (BL41XU)	SPring-8 (BL45XU)
Wavelength (Å)	1.0000	1.0000	1.0000
Space group	$P2_12_12_1$	$P2_12_12_1$	$P2_12_12_1$
Unit cell parameters			
a, *b*, *c* (Å)	57.4, 62.5, 83.1	57.5, 63.0, 83.4	56.2, 62.9, 82.0
α, β, γ (°)	90, 90, 90	90, 90, 90	90, 90, 90
Resolution (Å)	47.35–1.16 (1.18–1.16)	47.32–1.38 (1.40–1.38)	46.33–1.39 (1.41–1.39)
Number of unique reflections	101566 (4675)	62992 (3135)	59149 (2987)
R_{merge}[a]	0.034 (0.455)	0.131 (1.17)	0.018 (0.189)
R_{meas}	0.037 (0.502)	0.137 (1.24)	0.026 (0.268)
Completeness (%)	97.0 (91.4)	99.9 (97.8)	100.0 (99.5)
$\langle I/\sigma(I)\rangle$	23.1 (3.3)	10.9 (1.0)	24.8 (3.9)
$CC_{1/2}$	0.999 (0.893)	0. 998 (0.865)	0.999 (0.856)
Redundancy	6.4 (5.6)	1.0 (1.0)	1.9 (1.8)
Refinement			
Program	REFMAC 5.8	REFMAC 5.8	REFMAC 5.8
Resolution (Å)	41.71–1.16 (1.19–1.16)	47.32–1.38 (1.42–1.38)	46.37−1.39 (1.43−1.39)
Number of reflections	96318 (6650)	59812 (4306)	56262 (4089)
R_{work}[b]	0.197 (0.245)	0.165 (0.278)	0.207 (0.291)
R_{free}[b]	0.206 (0.266)	0.205 (0.289)	0.234 (0.325)
Completeness (%)	96.7 (91.9)	99.9 (98.4)	100.0 (99.6)
Number of atoms in an asymmetric unit			
Protein	2390	2397	2398
Water	318	298	235
Heme	86	86	86
Average *B* factors (Å^2)			
Protein	17.0	23.7	26.0
Water	24.3	28.7	31.1
Heme	12.4	18.8	20.0
Ramachandran plot (%)			
Favored	98.01	98.01	98.68
Allowed	1.99	1.99	1.32
Outlier	0.00	0.00	0.00

Statistics for the highest-resolution shell are given in parentheses.

[a] $R_{merge}=\Sigma_{hkl} \mid I - \langle I\rangle \mid (\Sigma_{hkl} \mid I \mid)^{-1}$.

[b] $R_{work}=\Sigma_{hkl} \mid \mid F_{obs} \mid - k \mid F_{calc} \mid \mid (\Sigma_{hkl} \mid F_{obs} \mid)^{-1}$, k: scaling factor. R_{free} was computed identically, except where all reflections belong to a test set of 5 % of randomly selected data.

Table S3. Molecular extinction coefficients at 408 nm of WT and mutant Mb monomers and dimers.[a]

Mb protein	$\varepsilon_{408\ nm}$ ($mM^{-1}\ cm^{-1}$)	
	monomer	dimer
WT Mb*	188	188
K_3A_2H Mb	181	181
K_3A_2H-L137E Mb	178	181
K_3A_2H-L137D Mb	180	180

[a] in 50 mM potassium phosphate buffer, pH 7.0.

Table S4. The dimer ratios at equilibriums for mutant Mbs at various temperatures.

Temperature (°C)	K_3A_2H Mb (%)	K_3A_2H-L137E Mb (%)	K_3A_2H-L137E Mb (%)
63.5	95.1 ± 0.4		
65.4	94.6 ± 0.2		
67.5	93.7 ± 0.2		
69.5	92.9 ± 0.3		
67.2		92.2 ± 0.3	96.1 ± 0.2
69.5		90.2 ± 0.4	93.6 ± 0.3
71.3		87.5 ± 0.3	91.3 ± 0.4
73.1		83.6 ± 0.3	86.7 ± 0.3